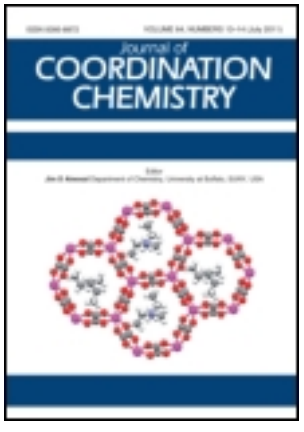

Journal of Coordination Chemistry
Publication details, including instructions for authors and subscription information:
http://www.tandfonline.com/loi/gcoo20

Square planar palladium(II) complexes of bipyridines: synthesis, characterization, and biological studies

Mohan N. Patel [a] , Promise A. Dosi [a] & Bhupesh S. Bhatt [a]
[a] Department of Chemistry, Sardar Patel University, Vallabh Vidyanagar 388 120, Gujarat, India
Accepted author version posted online: 04 Sep 2012.Version of record first published: 18 Sep 2012.

To cite this article: Mohan N. Patel , Promise A. Dosi & Bhupesh S. Bhatt (2012): Square planar palladium(II) complexes of bipyridines: synthesis, characterization, and biological studies, Journal of Coordination Chemistry, 65:21, 3833-3844

To link to this article: http://dx.doi.org/10.1080/00958972.2012.727207

Journal of Coordination Chemistry
Vol. 65, No. 21, 10 November 2012, 3833–3844

Square planar palladium(II) complexes of bipyridines: synthesis, characterization, and biological studies

MOHAN N. PATEL*, PROMISE A. DOSI and BHUPESH S. BHATT

Department of Chemistry, Sardar Patel University,
Vallabh Vidyanagar 388 120, Gujarat, India

(*Received 13 April 2012; in final form 30 July 2012*)

A series of square planar mononuclear palladium(II) complexes, $[Pd(L^n)(OMe)_2]$ (where L^n = 4-(4-chlorophenyl)-6-phenyl-2,2′-bipyridine, 4,6-bis(4-chlorophenyl)-2,2′-bipyridine, 4-(4-bromophenyl)-6-(4-chlorophenyl)-2,2′-bipyridine, and 6-(4-chlorophenyl)-4-*p*-tolyl-2,2′-bipyridine), have been synthesized and characterized. Interaction of palladium complexes with DNA has been investigated by electronic absorption spectra, viscosity measurements and DNA melting temperature techniques. The metal complex-DNA interaction produced hypochromism and bathochromism, suggesting intercalative binding. Viscosity data support the intercalation mode of binding. Palladium(II) complexes promote cleavage of plasmid pUC19 DNA from the supercoiled form to the open circular form. Antibacterial activities of the complexes have also been evaluated against five pathogenic bacteria. The antimicrobial test results reveal that all compounds have good antibacterial activity against both Gram(−ve) and Gram(+ve) bacterial species compared to the ligands and metal salt.

Keywords: Square planar; Palladium(II); Intercalation; pUC19; CT DNA

1. Introduction

Reactivity of palladium(II) complexes is of particular interest because these systems are rapidly reacting prototypes for platinum(II) complexes [1]. Platinum compounds are the most efficacious metal-based anticancer agents [2]. However, because of severe side effects, drug resistance and the limited spectrum of tumors [2], there has been a search for related complexes (e.g. Pd, Ru, and Au) that are able to improve effectiveness and reduce side effects of platinum-based drugs [3, 4]. Special attention in this regard has been given to palladium(II) complexes [5–8], since the coordination geometry and complex forming processes of palladium(II) are very similar to those of platinum(II).

DNA intercalation is a reversible non-covalent interaction originally proposed by Lerman [9] to account for the affinity of some small planar aromatic molecules for double-stranded DNA. This interaction consists of insertion of a drug molecule between two adjacent base pairs of the nucleic acid. Many workers [10] believe that intercalation is an important intermediate state in mutagenesis and carcinogenesis caused by a number of small molecules; it is also thought [11] that intercalation is part

*Corresponding author. Email: jeenen@gmail.com

ISSN 0095-8972 print/ISSN 1029-0389 online © 2012 Taylor & Francis
http://dx.doi.org/10.1080/00958972.2012.727207

of the mode of action of some antibacterial and antineoplastic medicines. Because of this, a large number of studies [12] on intercalation have been performed; studies on DNA intercalation by square-planar complexes [13] have appeared, although systematic structural variations have not been reported.

Continuing our interest in metal complexes [14], we report synthesis and characterization of new Pd(II) complexes. The complexes have been tested for their antibacterial activity against five microorganisms. All the complexes have been tested for their ability to bind to calf-thymus (CT) DNA. The binding properties of the complexes with CT DNA have been investigated with absorption titration, viscosity and DNA melting temperature experiments. The cleavage properties of the complexes have been performed using gel electrophoresis.

2. Experimental

2.1. *Materials*

Sodium tetrachloropalladate(II) was purchased from Chemport (India). *p*-Chloro acetophenone, *p*-bromo acetophenone, *p*-methyl acetophenone, acetophenone, *p*-chloro benzaldehyde, and 2-acetylpyridine were purchased from Spectrochem (Mumbai, India). Agarose, EB, TAE (Tris-acetyl-EDTA), bromophenol blue and xylene cyanol FF were purchased from Himedia (India). CT DNA was purchased from Sigma Chemical Co. (India). Culture of pUC19 bacteria (MTCC 47) was purchased from the Institute of Microbial Technology (Chandigarh, India).

2.2. *Physical measurements*

C, H, and N elemental analyses were performed with a VarioMICRO superuser elementar analysensysteme GmbH. Infrared spectra were recorded on a Fourier transform IR (FTIR) ABB Bomen MB 3000 spectrophotometer as KBr pellets from 4000 to 400 cm^{-1}. ^{1}H and ^{13}C NMR spectra were recorded on a Bruker Avance (400 MHz). Fast atomic bombardment mass spectra (FAB MS) were recorded on a Jeol SX 102/Da–600 mass spectrophotometer/data system using Argon/Xenon (6 kV, 10 mA) as the FAB gas. The accelerating voltage was 10 kV and spectra were recorded at room temperature. Electronic spectra were recorded on a UV–160 A UV-Vis spectrophotometer, Shimadzu (Japan). Photo quantization of the gel after electrophoresis was carried out on AlphaDigiDoc^{TM} RT. Version V.4.0.0 PC–Image software.

2.3. *Synthesis of ligands*

Substituted bipyridines, i.e. 4-(4-Xphenyl)-6-phenyl-2,2′-bipyridines, were synthesized by reacting 1-[2-oxo-2-(2-pyridyl)ethyl]pyridiniumiodide and 3-(4-Xphenyl)-1-phenyl-prop-2-en-1-one [15]. The reactant 1-[2-oxo-2-(2-pyridyl)ethyl]pyridinium iodide was prepared using 2-acetylpyridine, iodine, and pyridine [16], and 3-(4-Xphenyl)-1-phenylprop-2-en-1-one (X = chloro/bromo/methyl) was prepared *via* aldol condensation between substituted acetophenones and *p*-chloro benzaldehyde.

2.3.1. 4-(4-Chlorophenyl)-6-phenyl-2,2′-bipyridine (L^1). An excess of ammonium acetate (approximately 10 equiv) was added to a mixture of 3-(4-chlorophenyl)-1-phenylprop-2-en-1-one (2.88 mmol) and 1-[2-oxo-2-(2-pyridyl)ethyl]pyridinium iodide (2.88 mmol) in methanol (20 mL). After refluxing for 5–7 h, the reaction mixture was allowed to cool which led to the formation of greenish yellow needles of pure product. The solid was filtered off, washed with cold methanol, dried under vacuum and further recrystallized using hexane. A further crop of the desired product was obtained upon refluxing the filtrate for another 5–6 h and subsequent workup.

Yield: 54%, m.p. 140°C, mol. wt. 342.82. Anal. Calcd for $C_{22}H_{15}ClN_2$ (%): C, 77.08; H, 4.41; N, 8.17, found (%): C, 76.90; H, 4.47; N, 8.08. ^{1}H NMR ($CDCl_3$, 400 MHz): δ (ppm) 8.754–8.710 (complex, 2H, $H_{3',6'}$), 8.659 (s, 1H, H_3), 8.220 (d, 2H, $H_{2'',6''}$), 7.960 (s, 1H, H_5), 7.910 (t, 1H, $H_{4'}$), 7.789 (d, 2H, $H_{2'',6''}$), 7.578–7.474 (complex, 5H, $H_{3'',5'',3''',4''',5'''}$), 7.386 (t, 1H, $H_{5'}$), ^{13}C NMR ($CDCl_3$, 100 MHz): δ (ppm) 157.43 (C_6), 155.86 (C_2), 150.22 ($C_{2'}$), 149.09 (C_4), 147.22 ($C_{6'}$), 139.28 ($C_{1'}$), 138.25 ($C_{1''}$), 137.08 ($C_{4'}$), 129.92 ($C_{4''}$), 129.30 ($C_{2''',6'''}$), 128.80 ($C_{2'',6''}$), 128.55 ($C_{3''',5'''}$), 127.10 ($C_{3'',5''}$), 124.08 ($C_{4''}$), 121.78 ($C_{5'}$), 118.40 ($C_{3'}$), 117.50 (C_3), 102.75 (C_5). FT-IR (KBr, cm^{-1}): ν(C–H), 3012 (m); ν(C=C), 1538 (s); ν(C=N), 1459 (s); ν(C–H), 1047; δ (C–H), 725 (s).

2.3.2. 4,6-Bis(4-chlorophenyl)-2,2′-bipyridine (L^2). The ligand was synthesized using 1,3-bis(4-chlorophenyl)prop-2-en-1-one. Yield: 51%, m.p. 149°C, mol. wt. 377.27. Anal. Calcd for $C_{22}H_{14}Cl_2N_2$ (%): C, 70.04; H, 3.74; N, 7.43, found (%): C, 69.96; H, 3.68; N, 7.36. ^{1}H NMR ($CDCl_3$, 400 MHz): δ (ppm) 8.741 (dd, 1H, $H_{3'}$), 8.682–8.641 (complex, 2H, $H_{6',5}$), 8.169 (d, 2H, $H_{2''',6'''}$), 8.133–7.830 (complex, 2H, $H_{3,4'}$), 7.773 (d, 2H, $H_{2'',6''}$), 7.531–7.510 (complex 4H $H_{3'',5'',3''',5'''}$), 7.413 (dt, 1H, $H_{5'}$), ^{13}C NMR ($CDCl_3$, 100 MHz): δ (ppm) 156.51 (C_6), 156.10 (C_2), 155.97 ($C_{2'}$), 149.24 (C_4), 149.09 ($C_{6'}$), 137.74 ($C_{1''}$), 137.10 ($C_{4'}$), 136.97 ($C_{1'''}$), 135.34 ($C_{4'''}$), 129.64 ($C_{4''}$), 129.28 ($C_{3''',5'''}$), 128.95 ($C_{3'',5''}$), 128.53 ($C_{2''',6'''}$), 128.38 ($C_{2'',6''}$), 124.04 ($C_{5'}$), 121.54 ($C_{3'}$), 117.97 (C_3), 117.53 (C_5), FT-IR (KBr, cm^{-1}): ν(C–H), 3155 (m); ν(C=C), 1554 (s); ν(C=N), 1457 (s); ν(C–Cl), 1045; δ (C–H), 717 (s).

2.3.3. 4-(4-Bromophenyl)-6-(4-chlorophenyl)-2,2′-bipyridine (L^3). The ligand was synthesized using 3-(4-bromophenyl)-1-(4-chlorophenyl)prop-2-en-1-one. Yield: 59%, m.p. 156°C, mol. wt. 421.72. Anal. Calcd for $C_{22}H_{14}BrClN_2$ (%): C, 62.66; H, 3.35; N, 6.64, found (%): C, 62.73; H, 3.29; N, 6.57. ^{1}H NMR ($CDCl_3$, 400 MHz): δ (ppm) 8.732 (dd, 1H, $H_{3'}$), 8.662–8.616 (complex, 2H, $H_{6',5}$), 8.148 (d, 2H, $H_{2''',6'''}$), 7.870 (d, 2H, $H_{2'',6''}$), 7.803–7.772 (complex, 2H, $H_{4',5'}$), 7.502 (d, 2H, $H_{3''',5'''}$), 7.282 (s, 1H, H_3), 7.249 (d, 2H, $H_{3'',5''}$). ^{13}C NMR ($CDCl_3$, 100 MHz): δ (ppm) 156.43 (C_6), 156.02 (C_2), 155.94 ($C_{2'}$), 149.34 (C_4), 149.10 ($C_{6'}$), 137.75 ($C_{1''}$), 136.91 ($C_{4'}$), 135.27 ($C_{1'''}$), 134.68 ($C_{4'''}$), 129.05 (C_5), 128.97 ($C_{3''',5'''}$), 128.92 ($C_{3'',5''}$), 128.32 ($C_{2''',6'''}$), 123.97 ($C_{2'',6''}$), 121.47 ($C_{5'}$), 117.93 ($C_{3'}$), 117.55 (C_3), 116.16 ($C_{4''}$), FT-IR (KBr, cm^{-1}): ν(C–H), 3029 (m); ν(C=C), 1555 (s); ν(C=N), 1516 (s); ν(C–Cl), 1049 (s); ν(C–Br), 1025; δ (C–H), 750.

2.3.4. 6-(4-Chlorophenyl)-4-p-tolyl-2,2′-bipyridine (L^4). The ligand was synthesized using 1-(4-chlorophenyl)-3-*p*-tolylprop-2-en-1-one. Yield: 57%, m.p. 138°C, mol. wt. 356.11. Anal. Calcd for $C_{23}H_{17}ClN_2$ (%): C, 77.41; H, 4.80; N, 7.85, found (%): C, 77.35; H, 4.75; N, 7.79. ^{1}H NMR ($CDCl_3$, 400 MHz): δ (ppm) 8.743–8.695 (complex,

2H, $H_{3',6'}$), 8.598 (s, 1H, H_5), 8.122 (d, 1H, $H_{2'',6''}$), 7.930–7.870 (complex, 2H, $H_{3,4'}$), 7.775 (d, 2H, $H_{2'',6''}$), 7.508 (d, 2H, $H_{3'',5''}$), 7.385–7.350 (complex, 3H, $H_{3'',5'',5'}$), 2.470 (s, 3H, methyl), ^{13}C NMR ($CDCl_3$, 100 MHz): δ (ppm) 157.32 (C_6), 156.31 ($C_{2'}$), 156.25 ($C_{2'}$), 149.02 (C_4), 148.92 ($C_{6'}$), 139.24 ($C_{1''}$), 137.33 ($C_{4'}$), 136.92 ($C_{1''}$), 136.53 ($C_{4''}$), 135.14 ($C_{3'}$), 129.50 ($C_{3'',5''}$), 129.21 ($C_{3''5''}$), 128.53 ($C_{2'',6''}$), 126.95 ($C_{2'',6''}$), 123.87 ($C_{5'}$), 121.56 ($C_{4''}$), 117.86 (C_3), 116.96 (C_5), 21.33 (methyl), FT-IR (KBr, cm^{-1}): ν(C–H), 3063 (m); ν(C=C), 1574 (s); ν(C=N), 1535 (s); ν(C–Cl), 1045 (s); δ (C–H), 733 (m).

2.4. *Synthesis of complexes*

2.4.1. [Pd(L^1)($OMe)_2$] (1). All the complexes were synthesized by following the literature procedure [17]. 4-(4-Chlorophenyl)-6-phenyl-2,2′-bipyridine (0.5 mmol) in methanol and Na_2PdCl_4 (0.5 mmol) in distilled water (50 mL) were refluxed for 5 h. Reaction mixture was allowed to cool to room temperature and filtered. The obtained yellow product was washed with hot water and dried under vacuum. General reaction scheme for the synthesis of complexes is given in scheme 1. Yield: 63.7%, m.p.: 205°C, anal. Calcd for $C_{24}H_{21}ClN_2O_2Pd$, m.w. (%): 511.31, elemental anal. Calcd (%): C, 56.38; H, 4.14; N, 5.48; Pd, 20.81, found (%): C, 56.29; H, 4.08; N, 5.52; Pd, 20.73. FT-IR (KBr, cm^{-1}): ν(C–H) 3055 (m); ν(C=C) 1574 (s); ν(C=N) 1489 (s); ν(OMe), 1250; ν(C–Cl), 1040; δ (C–H) 741 (s); ν(M–O), 589; ν(M–N) 545 (s).

2.4.2. [Pd(L^2)($OMe)_2$] (2). Compound **2** was prepared using 4,6-bis(4-chlorophenyl)-2,2′-bipyridine. Yield: 63.5%, m.p.: 217°C, anal. Calcd for $C_{24}H_{20}Cl_2N_2O_2Pd$, m.w. (%): 545.75, elemental anal. Calcd (%): C, 52.82; H, 3.69; N, 5.13; Pd, 19.50, found (%): C, 52.88; H, 3.57; N, 5.08; Pd, 19.43. FT-IR (KBr, cm^{-1}): ν(C–H) 3055 (m);

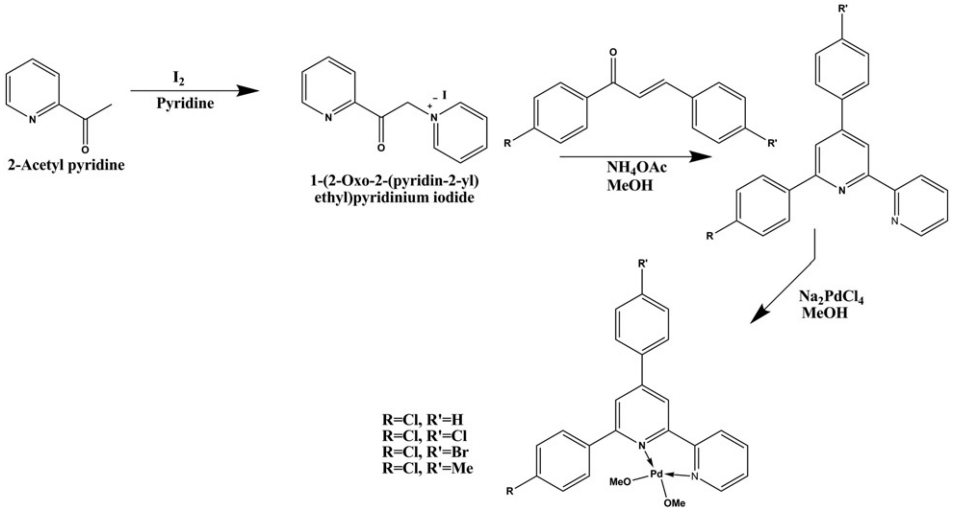

Scheme 1. General reaction scheme for synthesis of ligand and its Pd(II) complexes.

ν(C=C) 1582 (s); ν(C=N) 1481 (s); ν(OMe), 1257; ν(C–Cl), 1035; δ (C–H) 733 (s); ν(M–O), 585; ν(M–N) 543 (s).

2.4.3. [Pd(L^3)$(OMe)_2$] (3). Compound **3** was prepared using 4-(4-bromophenyl)-6-(4-chlorophenyl)-2,2′-bipyridine. Yield: 62.9%, m.p.: 227°C, anal. Calcd for $C_{24}H_{20}BrClN_2O_2Pd$, m.w. (%): 590.20, elemental anal. Calcd (%): C, 48.84; H, 3.42; N, 4.75; Pd, 18.03, found (%): C, 48.88; H, 3.35; N, 4.68; Pd, 17.96. FT-IR (KBr, cm^{-1}): ν(C–H) 3055 (m); ν(C=C) 1605 (s); ν(C=N) 1543 (s); ν(OMe), 1242; ν(C–Cl), 1042; ν(C–Br), 1022 δ (C–H) 771 (s); ν(M–O), 640; ν(M–N), 550 (s).

2.4.4. [Pd(L^4)$(OMe)_2$] (4). Compound **4** was prepared using 6-(4-chlorophenyl)-4-*p*-tolyl-2,2′-bipyridine. Yield: 65.3%, m.p.: 217°C, anal. Calcd for $C_{25}H_{23}ClN_2O_2Pd$, m.w. (%): 525.34, elemental anal. Calcd (%): C, 57.16; H, 4.41; N, 5.33; Pd, 20.26, found (%): C, 57.23; H, 4.35; N, 5.27; Pd, 20.19. FT-IR (KBr, cm^{-1}): ν(C–H) 3055 (m); ν(C=C), 1597 (s); ν(C=N) 1551 (s); ν(OMe), 1227; 1043; ν(C–Cl), 1043; δ (C–H) 741 (s); ν(M–O), 594; ν(M–N), 555 (s).

2.5. *Antibacterial activity*

The *in-vitro* antibacterial activities of metal salt, ligands, and palladium complexes were tested against three Gram(−ve); *Serratia marcescens* (MTCC 7103), *Escherichia coli* (MTCC 433), *Pseudomonas aeruginosa* (MTCC P09), and two Gram(+ve); *Staphylococcus aureus* (MTCC 3160), *Bacillus subtilis* (MTCC 7193), microorganisms. Solution of the complexes was prepared in DMSO. The minimum inhibitory concentration of each compound was defined as the lowest concentration exhibiting no visible growth. Luria Broth was employed as the bacteria growth medium. Serial concentrations of each of the tested compounds from 71 to 2800 μmol L^{-1} were prepared for the determination of MIC and inoculated with five different microorganisms. After incubation at 37°C for 24 h, the solution without turbidity was determined as the minimum inhibitory concentration.

2.6. *Absorption titration*

The UV absorbance at 260 and 280 nm of the CT DNA solution in 5 mmol L^{-1} Tris-HCl buffer (pH 7.2) gave a ratio of ~1.9, indicating the DNA was free of protein. The concentration of CT DNA was measured from the band intensity at 260 nm with the known ε value (6600 mol L^{-1} cm^{-1}). Absorption titration experiments were performed by maintaining the palladium complex concentration constant at 20 μmol L^{-1} while varying the concentration of CT DNA within 50–150 μmol L^{-1}. While measuring the absorption spectra, an equal quantity of CT DNA was added to both the complex solution and the reference solution to eliminate the absorbance of CT DNA itself. From the absorption data, the intrinsic binding constant K_b was determined from a plot of [DNA]/($\varepsilon_a - \varepsilon_f$) *versus* [DNA] using the following equation:

$$\frac{[DNA]}{(\varepsilon_a - \varepsilon_f)} = \frac{[DNA]}{(\varepsilon_b - \varepsilon_f)} + \frac{1}{K_b(\varepsilon_b - \varepsilon_f)}$$

where [DNA] is the concentration of CT DNA in base pairs. The apparent absorption coefficients ε_a, ε_f, and ε_b correspond to $A_{obsd.}/[Pd(II)]$, the extinction coefficient for the free palladium(II) complex and extinction coefficient for the palladium(II) complex in the fully bound form, respectively [18]. K_b is given by the ratio of slope to the intercept.

2.7. *DNA melting experiments*

DNA melting experiments were carried out by monitoring the absorption intensity of CT DNA (100 μmol L^{-1}) at 260 nm at various temperatures, both in the absence and presence of the palladium(II) complexes (20 μmol L^{-1}). Measurements were carried out using a Perkin–Elmer Lambda 35 spectrophotometer equipped with a Peltier temperature-controlling programmer (PTP 6) (±0.1°C) increasing the temperature of the solution by 0.5°C^{-1}.

2.8. *Viscosity measurements*

Viscometric titrations were performed with a Cannon-Ubbelohde viscometer. The viscometer was thermostated at 27°C (±0.1) in a constant temperature bath. The concentration of CT DNA was 200 μmol L^{-1} in NP and flow times were measured with an automated timer; each sample was measured three times and an average flow time was calculated. Data were presented as $(\eta/\eta_0)^{1/3}$ *versus* [complex]/[DNA], where η is the viscosity of DNA in the presence of complex and η_0 that of DNA alone. Viscosity values were calculated from the observed flowing time of DNA-containing solutions (t) corrected for that of buffer alone (t_0), $\eta = (t - t_0)$.

2.9. *Gel electrophoresis technique*

Gel electrophoresis of plasmid DNA (pUC19 DNA) was carried out in TE buffer with 15 μL reaction mixture containing 300 μg mL^{-1} plasmid DNA (10 mmol L^{-1} Tris, 1 mmol L^{-1} EDTA, pH 8.0) and 150 μmol L^{-1} complex. Reactions proceeded for 3 h at 37°C. All reactions were quenched by the addition of 5 μL loading buffer (40% sucrose, 0.2% bromophenol blue). The aliquots were loaded onto 1% agarose gel and electrophoreses occurred at 50 V in 1X TAE buffer. Gel was stained with 0.5 μg m L^{-1} ethidium bromide and photographed on a UV illuminator. The percentage of each form of DNA was quantified using AlphaDigiDoc™ RT Version V.4.1.0 PC–Image software. The degree of DNA cleavage activity was expressed as percentage cleavage of SC-DNA according to the following equation:

$$\%\text{DNA cleavage} = \frac{(\%\text{ of SC} - \text{DNA})\text{ control} - (\%\text{ of SC} - \text{DNA})\text{ sample}}{(\%\text{ of SC} - \text{DNA})\text{ control}}$$

3. Results and discussion

3.1. *Electronic spectra and magnetic moments*

In electronic spectra, the low-spin square-planar d^8 metal complexes are expected to give three spin allowed *d–d* transitions from the lower laying $d_{z^2} \rightarrow d_{xz}$, d_{yz}, $d_{z^2} \rightarrow d_{xy}$, and $d_{z^2} \rightarrow d_{x^2-y^2}$ [19].

In the synthesized palladium(II) complexes, only one *d–d* band is observed at ~438 nm, which is assigned to the $d_{z^2} \rightarrow d_{x^2-y^2}$ transition, with the other two bands masked by high intensity charge transfer bands. The bands at ~280 and ~260 nm correspond to charge transfer transitions. All these bands point to low-spin complex of the d^8 system with square planar geometry. The synthesized complexes were diamagnetic.

3.2. *IR spectra*

Aromatic C–H stretching and out of plane bending vibrations give bands at 740 and 3050 cm^{-1}. Very strong bands at ~1500 and ~1550 cm^{-1} for the C=N and C=C highest-energy pyridine-ring vibration of the ligands are shifted by 30–40 cm^{-1} to higher frequencies after complexation. The band for OMe is observed at ~1250 cm^{-1} and indicates OMe in the compound. The coordinate covalent bonding of the metal *via* nitrogen of bipyridine is supported by a sharp band at ~550, characteristic of Pd–N, suggesting that nitrogen of pyridine is coordinated [20]. The characteristic band for Pd–O is at ~600 cm^{-1}, which suggests that the OMe is directly attached to palladium [21].

3.3. *Mass spectrometry*

FAB MS spectrum of **1** was obtained using *m*–nitro benzyl alcohol as matrix (Supplementary material). Peaks at 136, 137, 154, 289, and 307 *m/z* values are of the matrix. The molecular ion peak for complex is observed at 512 *m/z* (I) and peaks corresponding to the fragments $[M–OMe]^+$, $[M–2(OMe)]^+$, and 4-(4-chlorophenyl)-6-phenyl-2,2′-bipyridine are observed at 481 (II), 448 (III), and 342 (IV) *m/z*, respectively. The fragmentations of phenyl and *p*-chlorophenyl from 4-(4-chlorophenyl)-6-phenyl-2,2′-bipyridine shows peaks at 265 (V) and 231 (VI) *m/z*, respectively. The peak corresponding to 2,2′-bipyridine is observed at 154 (VII) *m/z*. Doublets exist at 512 : 514, 481 : 483, 448 : 450, and 265 : 267 *m/z*, which correspond to isotopic patterns of chlorine. Moreover, peaks due to species containing the isotope of palladium were easily detected at *m/z*: 508, 510, 511, 512, 514, and 516 for fragment I; 476, 478, 480, 481, 483, and 485 for fragment II; and 444, 446, 447, 448, 450, and 452 for fragment III of ^{102}Pd, ^{104}Pd, ^{105}Pd, ^{106}Pd, ^{108}Pd, and ^{110}Pd, respectively (figure 1) [22]. The mass fragmentation pattern is shown in "Supplementary material."

3.4. *Antibacterial activity*

A comparative study of the MIC values of the ligands and their complexes indicates that the metal complexes show better activity against three Gram(−ve) and two Gram(+ve) microorganisms compared to the bidentate ligands and metal salts (table 1). Complexes **1** and **2** show better antibacterial activity than **3** and **4**. Complex **2** is more

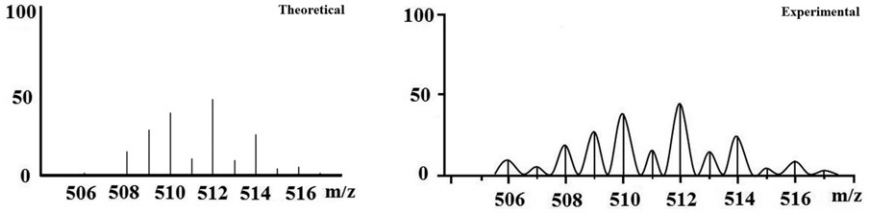

Figure 1. Experimental and theoretical isotope patterns of FAB-MS for **1**.

Table 1. Minimum inhibitory concentration of palladium complexes (μmol L^{-1}).

Compounds	*S. aureus*	*B. subtilis*	*S. marcescens*	*P. aeruginosa*	*E. coli*
Na_2PdCl_4	2238.00	2490.00	2145.00	1940.00	2820.00
Ligand 1 (L^1)	610	705	670	645	675
Ligand 2 (L^2)	540	510	585	490	535
Ligand 3 (L^3)	610	595	650	625	635
Ligand 4 (L^4)	670	715	720	720	725
$[Pd(L^1)(OMe)_2]$ (**1**)	88	89	91	92	88
$[Pd(L^2)(OMe)_2]$ (**2**)	77	74	71	79	78
$[Pd(L^3)(OMe)_2]$ (**3**)	82	84	82	81	80
$[Pd(L^4)(OMe)_2]$ (**4**)	99	104	102	98	99

potent because of the presence of two electronegative chlorines in the bidentate ligand. The increase in antibacterial activity of the metal chelate can be explained by chelation theory [23]. Our complexes show higher antibacterial activity than Pd(II) complexes of tetracycline, doxycycline and chlortetracycline (MIC = 2.08–66.50 μmol L^{-1} against *E. Coli*) reported by Guerra *et al.* [24], but the complexes are less active than ciprofloxacin. Palladium complexes may deactivate various cellular enzymes, which play a role in various metabolic pathways of organisms [25].

3.5. *Absorption titration*

Absorption titration is a common way to investigate the interactions of complexes with DNA. We have used absorption titration method to monitor interaction of **1**–**4** with CT DNA. Intercalation of a complex to DNA generally results in hypochromism and red shift (bathochromism) (figure 2) of the absorption band due to strong π–π^* stacking interaction between the aromatic chromophore of the ligand and the base pairs of DNA [14]. The extent of hypochromism, thus gives an estimate of the strength of intercalation. The binding constants of the palladium complexes are 2.31×10^4, 4.76×10^4, 3.47×10^4, and 1.24×10^4 for **1**, **2**, **3**, and **4**, respectively. The complexes show higher binding constant values than [Pd(en)(8-QO)]Cl (1.7×10^3 at 300 K and 1.6×10^3 at 310 K) reported by Mansouri-Torshizi *et al.* [26].

3.6. *DNA denaturation experiments*

The binding of molecules into the double helix is known to increase the melting temperature. The melting temperature is the temperature at which the double helix

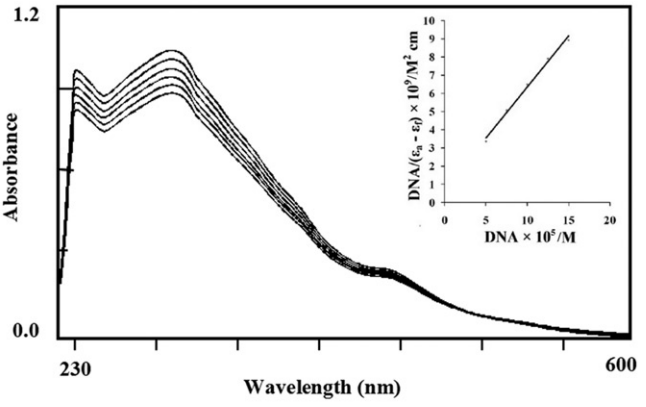

Figure 2. Absorption spectral traces of **1** with increasing amount of DNA in Tris-HCl buffer (50 mmol L^{-1} Tris-HCl, pH 7.2). [complex] = 20 μmol L^{-1}, [DNA] = 50–150 μmol L^{-1} with incubation period of 15 min at 37°C. Plots of [DNA]/($\varepsilon_a - \varepsilon_f$) *vs.* [DNA] for the titration of DNA with palladium(II) complexes.

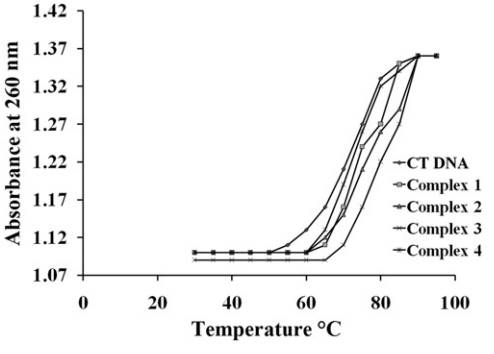

Figure 3. DNA melting temperature curves of CT DNA and palladium complexes in Tris-HCl buffer (50 mmol L^{-1} Tris-HCl, pH 7.2).

is denatured into single-stranded DNA. The extinction coefficient of DNA bases at 260 nm in the double-helical form is much lower than in the single-stranded form. Hence, melting of the helix leads to an increase in absorption at this wavelength. Thus, the transition temperature from helix to coil can be determined by monitoring the absorbance of the DNA base at 260 nm as a function of temperature.

The thermal denaturation experiment carried out for CT DNA in the absence of Pd(II) complexes revealed a T_m of 74.2°C under our experimental conditions (figure 3). On addition of the complexes, T_m of DNA increased to 78.1, 79.1, 78.6, and 77.8 for **1**, **2**, **3**, and **4**, respectively, at a concentration ratio [DNA]/[Pd] of 5 : 1. The increase (3.6–4.9) in T_m is comparable to that observed for classical intercalators [27]. Such DNA melting temperature studies of some mixed-ligand palladium(II) complexes were studied by Tercero *et al.* [28], who reported that the ΔT_m of the complexes increased by ~9.3°C and suggested the intercalative mode of binding.

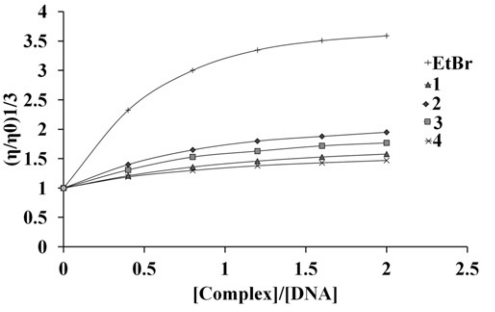

Figure 4. Effect on relative viscosity of DNA under the influence of increasing amount of ethidium bromide and complexes at 27 ± 0.1°C in Tris-HCl buffer (50 mmol L^{-1} Tris-HCl, pH 7.2).

3.7. *Viscosity measurements*

To investigate further, the binding modes of the complexes, viscosity measurements on solutions of CT DNA incubated with the complexes were carried out. Because the viscosity of a DNA solution is sensitive to the addition of drugs and metal complexes bound by intercalation, we examined the effect on the specific relative viscosity of DNA upon addition of the complexes. Since the relative specific viscosity (η/η_0) (η and η_0 are the specific viscosities of DNA in the presence and absence of the complexes, respectively) of DNA reflects the increase in contour length associated with separation of DNA base pairs caused by intercalation, a classical intercalator such as ETBr could cause a significant increase in viscosity of DNA solutions. In contrast, a partial and/or non-classical intercalation could bend or kink DNA resulting in a decrease in its effective length with a concomitant increase in its viscosity [29]. The plots of relative viscosities with [Pd]/[DNA] are shown in figure 4. The relative viscosity of DNA increases with increase in the concentration of the complexes but less compared to that of potential classical intercalators, e.g. ethidium bromide. Similar results were obtained for Pd(II) complexes reported by Ghosh *et al.* [30] and Nyarko *et al.* [31]. This is consistent with the observed trend by other optical methods and suggests primarily intercalation of the complex.

3.8. *Cleavage of pUC19 plasmid DNA by palladium(II) complexes*

Agarose gel electrophoresis is a convenient method to assess cleavage of DNA by metal complexes to assess the factors affecting the nucleolytic efficiency of a complex and to compare the nucleolytic property of different metal complexes. This has been done in this study with the $[Pd(L^n)(OMe)_2]$ complexes. DNA cleavage experiments were performed by agarose gel electrophoresis using plasmid pUC19 DNA (300 μmol L^{-1}) in 10 mmol L^{-1} Tris/1 mmol L^{-1} NaCl buffer (pH 8) and the palladium(II) complexes (figure 5). DNA cleavage data are given in table 2. The complexes show complete conversion of the SC (form I) to its nicked-circular form (NC, form II). Control experiments with DNA or palladium salt alone do not show any apparent conversion of SC to its NC form. Such cleavage ability of plasmid DNA by Pd(II) complexes was reported by Pérez-Cabré *et al.* [32] and Yodoshi and Okabe [33].

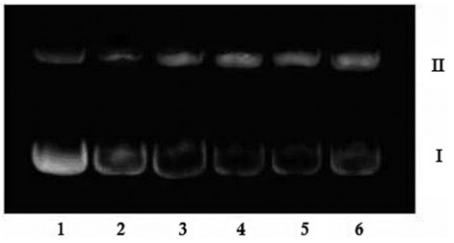

Figure 5. Photogenic view of interaction of pUC19 DNA ($300\,\mu g\,mL^{-1}$) with palladium(II) complexes ($200\,\mu mol\,L^{-1}$) using 1% agarose gel containing $0.5\,\mu g\,mL^{-1}$ ethidium bromide. All reactions were incubated in TE buffer (pH 8) in a final volume of 15 µL for 3 h at 37°C: Lane 1, DNA control; Lane 2, Na_2PdCl_4; Lane 3, [Pd(clpbpy)$(OMe)_2$] (**1**); Lane 4, [Pd(clcpbpy)$(OMe)_2$] (**2**); Lane 5, [Pd(brcpbpy)$(OMe)_2$] (**3**); and Lane 6, [Pd(clmpbpy)$(OMe)_2$] (**4**).

Table 2. Gel electrophoresis data of Pd(II) complexes.

Compounds	SC (%)	OC (%)	Cleavage (%)
DNA control	88.2	11.8	–
DNA + Na_2PdCl_4	70.8	20.8	19.77
DNA + **1**	29.1	70.8	67.00
DNA + **2**	17.4	82.6	80.27
DNA + **3**	23.1	76.1	73.80
DNA + **4**	36.9	43.1	58.16

4. Conclusion

Synthesis and characterization of four Pd(II) complexes with different bipyridines has been achieved. All complexes were more bacteriostatic than bipyridines and metal salt against five microorganisms. Binding behavior of the palladium chelates of bipyridines was subtly but distinctly different, depending on the structure of the bipyridines. As the electronegativity of the substituted group on bipyridine skeleton increases, the interaction becomes stronger. Increasing order for the DNA interaction behavior of synthesized complexes is **4** < **1** < **3** < **2** on the basis of K_b values, change in relative viscosity, change in melting temperature and the plasmid cleavage study.

Acknowledgments

Authors thank Head, Department of Chemistry, Sardar Patel University, India, for making it convenient to work in the laboratory and U.G.C. for providing financial support under ''UGC Research Fellowship for Meritorious Students'' scheme.

References

[1] U.K. Haring, R.B. Martin. *Inorg. Chim. Acta*, **78**, 259 (1983).
[2] S. Ahmad. *Chem. Biodivers.*, **7**, 543 (2010).

[3] A. Casini, C. Hartinger, C. Gabbiani, E. Mini, P.J. Dyson, B.K. Keppler, L. Messori. *J. Inorg. Biochem.*, **102**, 564 (2008).
[4] H.K. Liu, S.J. Berners-Price, F. Wang, J.A. Parkinson, J. Xu, J. Bella, P.J. Sadler. *Angew. Chem., Int. Ed.*, **45**, 8153 (2006).
[5] L. Tusek-Bozic, M. Juribasic, P. Traldi, V. Scarcia, A. Furlani. *Polyhedron*, **27**, 1317 (2008).
[6] A.I. Matesanz, P. Souza. *J. Inorg. Biochem.*, **101**, 1354 (2007).
[7] S. Padhye, Z. Afrasiabi, E. Sinn, J. Fok, K. Mehta, N. Rath. *Inorg. Chem.*, **44**, 1154 (2005).
[8] F. Shaheen, A. Badshah, M. Gielen, C. Gieck, M. Jamil, D. de Vos. *J. Organomet. Chem.*, **693**, 1117 (2008).
[9] L.S. Lerman. *J. Mol. Biol.*, **3**, 18 (1961).
[10] W.D. Wilson, R.L. Jones. In *Intercalation Chemistry*, M.S. Wittingham, A.J. Jacobson (Eds), pp. 445–501, Academic Press, New York (1982).
[11] W.D. Wilson, R.L. Jones. *Adv. Pharmacol. Chemother.*, **18**, 177 (1981).
[12] S. Neidle, L.H. Pearl, J.V. Skelly. *Biochemistry J.*, **243**, 1 (1987).
[13] W.I. Sundquist, S. Lippard. *Coord. Chem. Rev.*, **100**, 293 (1990).
[14] M.N. Patel, P.A. Dosi, B.S. Bhatt, V.R. Thakkar. *Spectrochim. Acta A*, **78**, 763 (2011).
[15] F. Neve, M. Ghedini, O. Francescangeli, S. Campagna. *Liq. Cryst.*, **24**, 673 (1998).
[16] S.M. Treffert-Ziemelis, J. Golus, D.P. Strommen, J.R. Kincaid. *Inorg. Chem.*, **32**, 3890 (1993).
[17] K.D. Hodges, J.V. Rund. *Inorg. Chem.*, **14**, 525 (1975).
[18] R.B. Nair, E.S. Teng, S.L. Kirkland, C.J. Murphy. *Inorg. Chem.*, **37**, 139 (1998).
[19] A.J. Bridgeman. *Inorg. Chem.*, **47**, 4817 (2008).
[20] J. Stawińska, M. Cieślak-Golonka, Z. Staszak, R. Gancarz. *Transition Met. Chem.*, **26**, 153 (2001).
[21] B. Miller, S. Wild, H. Zorbas, W. Beck. *Inorg. Chim. Acta*, **290**, 237 (1999).
[22] J. Zhang, L. Ma, F. Zhang, Z. Zhang, L. Li, S. Wang. *J. Coord. Chem.*, **65**, 239 (2012).
[23] H.M. Parekh, S.R. Mehta, M.N. Patel. *Russ. J. Inorg. Chem.*, **51**, 67 (2006).
[24] W. Guerra, E.A. Azevedo, A.R.S. Monteiro, M.B. Rodriguez, E.C. Souza, M.A. Nascimento, A.P.S. Fontes, L. Moyec, E.C. Pereira-Maia. *J. Inorg. Biochem.*, **99**, 2348 (2005).
[25] L.T. Yildrima, R. Kurtaran, H. Namli, A.D. Azaz, O. Atakol. *Polyhedron*, **26**, 4187 (2007).
[26] H. Mansouri-Torshizi, M. Saeidifar, G.R. Rezaei Behbehani, A. Divsalarc, A.A. Saboury. *J. Chin. Chem. Soc.*, **57**, 1299 (2010).
[27] G.A. Neyhart, N. Grover, S.R. Smith, W.A. Kalsbeck, T.A. Fairly, M. Cory, H.H. Thorp. *J. Am. Chem. Soc.*, **115**, 4423 (1993).
[28] J.M. Tercero, A. Matilla, M.A. Sanjuán, C.F. Moreno, J.D. Martín, J.A. Walmsley. *Inorg. Chim. Acta*, **342**, 77 (2003).
[29] T. Hirohama, Y. Kuranuki, E. Ebina, T. Sugizaki, H. Arii, M. Chikira, P.T. Selvi, M. Palaniandavar. *J. Inorg. Biochem.*, **99**, 1205 (2005).
[30] P.K. Ghosh, S. Saha, A. Mahapatra. *Polyhedron*, **26**, 2655 (2007).
[31] E. Nyarko, N. Hanada, A. Habib, M. Tabata. *Inorg. Chim. Acta*, **357**, 739 (2004).
[32] M. Pérez-Cabré, G. Cervantes, V. Moreno, M.J. Prieto, J.M. Pérez, M. Font-Bardia, X. Solans. *J. Inorg. Biochem.*, **98**, 510 (2004).
[33] M. Yodoshi, N. Okabe. *Chem. Pharm. Bull.*, **56**, 908 (2008).